J. Fluid Mech. (1989), *vol.* 200, *pp.* 77–93
Printed in Great Britain

Topographic waves in open domains. Part 2. Bay modes and resonances

By THOMAS F. STOCKER† AND E. R. JOHNSON‡

† Laboratory of Hydraulics, Hydrology and Glaciology, ETH Zürich, Switzerland.

‡ Department of Mathematics, University College London, Gower Street, London WC1E 6BT, UK

(Received 13 April 1988)

The topographic wave equation is solved in a domain consisting of a channel with a terminating bay zone. For exponential depth profiles the problem reduces to an algebraic eigenvalue problem. In a flat channel adjacent to a shelf-like bay zone the solutions form a countably infinite set of orthogonal bay modes: the spectrum of eigenfrequencies is purely discrete. A channel with transverse topography allows wave propagation towards and away from the bay: the spectrum has a continuous part below the cutoff frequency of free channel waves. Above this cutoff frequency a finite number (possibly zero) of bay-trapped solutions occur. Bounds for this number are given. At particular frequencies below the cutoff the system is in resonance with the incident wave. These resonances are shown to be associated with bay modes.

1. Introduction

Topographically trapped waves have been extensively studied in both open and closed domains. In open geometries they occur as shelf waves propagating along continental boundaries, accounting for a large portion of the kinetic energy of the coastal flow field. Observations have been well interpreted by analytical and numerical models. Topographic waves have also been identified and modelled in closed domains. Although this was successful for lakes with a circular shape, interpretation of long-periodic signals in an elongated lake demonstrated the limitation of the existing analytical models (Mysak *et al.* 1985; Johnson 1987*a*).

Stocker & Hutter (1986, 1987*a*, *b*) present extensive results from numerical integrations of a low-order spectral model for a rectangular lake with idealized topography. For their chosen depth profiles normal modes can be divided into two types: *basin-wide modes* for which the motion is spread throughout the lake and *bay modes* for which the motion is highly localized. The bay modes correspond to the high-frequency modes found in the finite-element model of the Swiss Lake of Lugano by Trösch (1984) and come closest to the observed frequencies.

Analytical models by Lamb (1932), Ball (1965), Mysak (1985) and Johnson (1987*a*) have concentrated on basin-wide modes. In fact, the conformal mapping results of Johnson (1987*b*) show that, with the exception of the Ball bathymetry, the topography in each model can be mapped to an along-shore invariant topography in a straight channel and hence cannot support localized modes. Basin-wide modes correspond to propagating shelf wave modes.

It is the purpose of the present paper to give a simple model that displays the bay modes and resonances found in the numerical results. Section 2 introduces the

geometry of a straight, semi-infinite channel with a shelf terminating in a bay zone formed by an oblique shelf. The problem of finding eigenfrequencies and eigenmodes is reduced to an algebraic eigenvalue problem. Upper and lower bounds and estimates of the eigenvalues are obtained by restricting consideration to the bay zone and applying suitable open boundary conditions. In §3 the special case of a bay zone adjacent to a flat channel is investigated. The spectrum of eigenfrequencies is countably infinite. The results are extended in §4 to channels with shelves allowing energy to leak from the bay. Here, the spectrum consists of a finite discrete part and a continuous part. An estimate of the size of the discrete spectrum is given. Results are summarized in §5.

2. Statement of the problem

Non-divergent, barotropic topographic waves on an f-plane are governed by the linearized equation for the conservation of potential vorticity (Rhines 1969*a*, *b*),

$$\frac{\partial}{\partial t}\nabla\cdot(H^{-1}\nabla\Psi)+\hat{\boldsymbol{z}}\cdot(\nabla\Psi\wedge\nabla H^{-1})=0 \quad \text{in } \mathscr{D}, \tag{2.1}$$

$$\Psi=0 \quad \text{on } \mathscr{D}, \tag{2.2}$$

where Ψ is the mass transport stream function, H is the local fluid depth, $\hat{\boldsymbol{z}}$ is the vertical unit vector and ∇ is the horizontal gradient operator. Time in (2.1) has been scaled on f^{-1}. The situations where (2.1) is a good model of geophysical motion are discussed briefly in Part 1 (Johnson 1989). Condition (2.2) expresses vanishing mass transport through the boundary $\partial\mathscr{D}$ of the domain.

Take Cartesian coordinates and consider the semi-infinite channel $x\geqslant 0, 0\leqslant y\leqslant 1$ with the depth profile

$$H(x,y)=\begin{cases}\mathrm{e}^{2b(x-l)+2c(y-1)}, & 0\leqslant x\leqslant l,\\ \mathrm{e}^{2c(y-1)}, & x>l.\end{cases} \tag{2.3}$$

Figure 1 displays the lines of constant depth for this geometry. Since $\log H$ is harmonic (2.1) reduces to a Helmholtz equation (Rhines & Bretherton 1973). Look for solutions of the form

$$\Psi=\mathrm{Re}\{\mathrm{e}^{-\mathrm{i}\sigma t}\psi\} \tag{2.4}$$

with non-dimensional frequency σ. Then with (2.3), (2.1) reduces in both regions to

$$\psi_{xx}+\psi_{yy}-2\beta\psi_x-2\gamma\psi_y=0,$$

where

$$\beta=\begin{cases}b+\mathrm{i}\dfrac{c}{\sigma}, & \\ \mathrm{i}\dfrac{c}{\sigma}, & \end{cases} \qquad \gamma=\begin{cases}c-\mathrm{i}\dfrac{b}{\sigma}, & 0\leqslant x\leqslant l,\\ c, & x>l.\end{cases} \tag{2.5}$$

Introducing

$$\psi(x,y)=\mathrm{e}^{\beta x+\gamma y}\phi(x,y)$$

gives

$$\phi_{xx}+\phi_{yy}+\kappa^2\phi=0, \tag{2.6}$$

where

$$\kappa^2=\begin{cases}(b^2+c^2)\left(\dfrac{1}{\sigma^2}-1\right), & 0\leqslant x\leqslant l,\\ c^2\left(\dfrac{1}{\sigma^2}-1\right), & x>l.\end{cases} \tag{2.7}$$

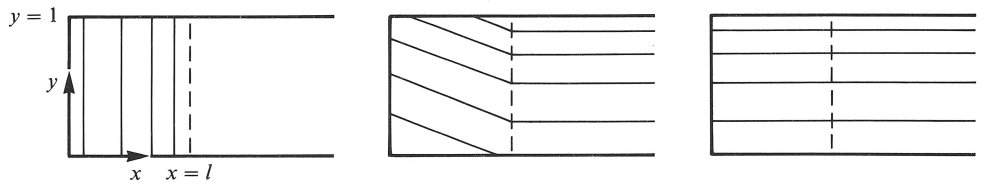

FIGURE 1. A semi-infinite channel in $x \geqslant 0, 0 \leqslant y \leqslant 1$ with a bay zone for $0 \leqslant x \leqslant l$ and an adjacent channel for $x > l$. Isobaths are given for three cases of b and c. In the bay they have slope $-bl/c$; (*a*) $b > 0$, $c = 0$; (*b*) $b > 0$, $c > 0$; (*c*) $b = 0$, $c > 0$.

Solutions of (2.1) in the semi-infinite channel can be obtained by solving (2.6) in the two regions and matching the transport and velocity field across $x = l$.

The boundary conditions on ϕ are

$$\phi = 0 \quad \text{on } \partial\mathscr{D}, \tag{2.8}$$

and the far-field condition that the kinetic energy remains bounded at infinity, i.e.

$$\nabla\phi \cdot \nabla\phi^* < \infty \quad \text{as } x \to \infty \tag{2.9}$$

when an asterisk denotes the complex conjugate. The fundamental solutions in the bay can be written

$$\phi_n^{\mathrm{b}} = \sinh \alpha_n x \sin n\pi y, \quad n = 1, 2, \ldots, \tag{2.10}$$

introducing for convenience

$$\alpha_n^2 = (n\pi)^2 - (b^2 + c^2)\left(\frac{1}{\sigma^2} - 1\right), \quad \hat{\alpha}_n^2 = -\alpha_n^2. \tag{2.11 a, b}$$

Here the superscript b stands for bay and n is the transverse mode number. The α_n are either real or purely imaginary. The ϕ_n^{b} satisfy (2.8) at $x = 0$ and $y = 0, 1$.

The corresponding fundamental modes in the channel can be written as

$$\phi_n^{\mathrm{c}} = \exp\left(\mathrm{i}\frac{c}{\sigma}x + \mathrm{i}k_n x\right)\sin n\pi y, \quad n = 1, 2, \ldots, \tag{2.12}$$

where the frequency σ is related to the along-channel wavenumber k via the dispersion relation

$$\sigma = \frac{2ck}{k^2 + c^2 + (n\pi)^2}, \tag{2.13}$$

i.e.

$$k_n = \frac{c}{\sigma} \pm \left[c^2\left(\frac{1}{\sigma^2} - 1\right) - (n\pi)^2\right]^{\frac{1}{2}}. \tag{2.14}$$

With these definitions k is the wavenumber in the x-direction of the stream function ψ. Propagating modes with transverse mode number n are possible provided that the frequency does not exceed the cutoff frequency of the nth transverse mode:

$$0 < \sigma < \sigma_n = \frac{c}{[c^2 + (n\pi)^2]^{\frac{1}{2}}}. \tag{2.15}$$

At frequencies $\sigma > \sigma_n$ the modes decay exponentially.

It is shown in Part 1 that bounds on the eigenfrequencies can be obtained by considering reduced domains with suitable boundary conditions. In the present

geometry it is convenient to take the reduced region to be the bay zone. As the channel alone cannot support trapped modes the eigenfrequencies of the reduced bay are in a one-to-one correspondence with those of the full problem. The boundary conditions at the bay edge associated with the upper, σ^{u}_{nm}, and lower, σ^{ℓ}_{nm}, bounds for the eigenfrequency of the (n,m)-mode are given by

$$\phi = 0 \quad \text{for } \sigma^{\ell}_{nm}, \qquad \phi_x + b\phi = 0 \quad \text{for } \sigma^{\mathrm{u}}_{nm}. \tag{2.16}$$

The eigenmodes can be written in the form

$$\phi = \sin \hat{\alpha}_m x \sin n\pi y, \quad m, n = 1, 2, \ldots,$$

with associated frequency estimates

$$\sigma^{\ell,\mathrm{u}}_{nm} = \frac{(b^2+c^2)^{\frac{1}{2}}}{(b^2+c^2+(n\pi)^2+\hat{\alpha}_m^2)^{\frac{1}{2}}}, \tag{2.17}$$

where $\hat{\alpha}_m = m\pi/l$ for σ^{ℓ}_{nm}, $\hat{\alpha}_m + b\tan\hat{\alpha}_m l = 0$ for σ^{u}_{nm}.

For use in §4 note that an explicit upper bound for σ^{u}_{nm} is given by

$$\hat{\alpha}_m = (m-\tfrac{1}{2})\pi/l. \tag{2.18}$$

The eigenfrequencies of the full and two reduced problems are thus countably infinite. The spectra are discrete with an accumulation point at $\sigma = 0$. The quality of the estimate (2.17) is shown below.

3. The flat channel

Consider a semi-infinite domain with a flat channel section, i.e. $c = 0$ in (2.3), see figure 1. There are no propagating waves in the channel: ψ decays exponentially there, with (2.14) giving $k = in\pi$. In the bay the depth profile in x allows shelf waves to propagate in the y-direction and be reflected from the channel walls $y = 0, 1$. The solution in this case can be written

$$\psi = \begin{cases} \sum_{n=1}^{\infty} a_n \psi^{\mathrm{b}}_n = \exp\left(bx - \mathrm{i}\frac{b}{\sigma}y\right) \sum_{n=1}^{\infty} a_n \sinh\alpha_n x \sin n\pi y, & 0 \leqslant x \leqslant l, \\ \sum_{n=1}^{\tilde{\infty}} d_n \psi^{\mathrm{c}}_n = \sum_{n=1}^{\tilde{\infty}} d_n \exp(-n\pi x)\sin n\pi y, & x > l, \end{cases} \tag{3.1}$$

with α_n given by (2.11) with $c = 0$. The stream function (3.1) with (2.4) is an exact solution of (2.1) in the semi-infinite channel provided the stream function and the velocity field are continuous across $x = l$. Since the set $\{\sin n\pi y, n = 1, 2, \ldots\}$ is complete in $[0, 1]$, this requirement determines the complex coefficients a_n and d_n of the superposition (3.1), viz.

$$\exp\left(bl - \mathrm{i}\frac{b}{\sigma}y\right) \Sigma a_n \sinh\alpha_n l \sin n\pi y = \Sigma d_n \exp(-n\pi l)\sin n\pi y, \tag{3.2a}$$

$$\exp\left(bl - \mathrm{i}\frac{b}{\sigma}y\right) \Sigma a_n (b\sinh\alpha_n l + \alpha_n \cosh\alpha_n l)\sin n\pi y$$

$$= \Sigma d_n (-n\pi)\exp(-n\pi l)\sin n\pi y. \tag{3.2b}$$

Operating with

$$\int dy \exp\left(\mathrm{i}\frac{b}{\sigma}y\right)\sin m\pi y$$

on both sides of (3.2) and using the orthogonality of $\sin n\pi y$ gives

$$\tfrac{1}{2}\mathrm{e}^{bl}a_m \sinh \alpha_m l = J_{mn}\, d_n\, \mathrm{e}^{-n\pi l}, \tag{3.3a}$$

$$\tfrac{1}{2}\mathrm{e}^{bl}a_m (b\sinh \alpha_m l + \alpha_m \cosh \alpha_m l) = J_{mn}\, d_n(-n\pi)\, \mathrm{e}^{-n\pi l}, \tag{3.3b}$$

where the sum over n is understood and the matrix elements J_{mn} are defined as

$$J_{mn} = \int_0^1 \mathrm{d}y \exp\left(\mathrm{i}\frac{b}{\sigma}y\right)\sin m\pi y \sin n\pi y$$

$$= \frac{2}{\pi}\tau(-1)^{m+n}\frac{mn}{((m+n)^2-\tau^2)(\tau^2-(m-n)^2)}\{\sin \pi\tau + \mathrm{i}(\cos \pi\tau - (-1)^{m+n})\}, \tag{3.4}$$

where $\tau = b/\pi\sigma$. Combining (3.3a) and (3.3b) leads to

$$D_{mn}\, \mathrm{e}^{-n\pi l}\, d_n = 0 \tag{3.5}$$

with

$$D_{mn} = (b + \alpha_m \coth \alpha_m l + n\pi) J_{mn}.$$

This has a non-trivial solution provided

$$\det \boldsymbol{D} = 0. \tag{3.6}$$

In order to obtain numerical solutions the infinite system (3.5) must be truncated. If the summation is restricted to $n = 1, \ldots, N$, (3.1) is merely an approximation to the true solution in that all transverse modes with mode numbers larger than N are discarded. The error is then orthogonal to all modes $n \leqslant N$, and completeness of the $\sin n\pi y$ implies convergence for increasing truncation order. The problem therefore reduces to solving the algebraic eigenvalue problem (3.5) of order N. Numerical calculations have revealed that (3.5) represents a fairly stiff system of equations. Equation (3.6) selects distinct eigenfrequencies for which there is wave motion in the bay region which exponentially decays outside. It has been demonstrated in Part 1 that the eigenvalues of the exact problem (2.1) are real. Generally, $\det \boldsymbol{D}$ takes complex values and one might wonder whether the truncated problems (3.6) also yield real eigenfrequencies σ. Indeed, it can easily be shown that the problem of lowest order ($N = 1$) requires real eigenfrequencies in order to satisfy (3.6). A similar result for $N > 1$ is not immediate, although computations suggest this is the case.

Table 1 lists the first four eigenfrequencies of a flat, semi-infinite channel with a shelf bay zone. The convergence of these values with increasing N is rapid; an accurate approximation is obtained with N as small as three. The coefficients show similar rapid convergence with increasing N. Table 2 shows that the approximations to a particular coefficient a_i in the expansion of the (1, 2) mode are well determined by $N = 7$ for $i \leqslant 4$.

Figure 2 displays the stream function for the first four eigenmodes. Wave energy is trapped within the bay region, propagating back and forth on the bay shelf. For $\sigma > 0$ (northern hemisphere) the waves are right bounded, i.e. their phase propagates in the negative y-direction. Outside the bay the stream function vanishes exponentially. The influence of the topography parameter b is shown in figure 3. Frequencies increase monotonically with b and approach 1 as b goes to infinity,

N	$(n,m) = (1,1)$	$(1,2)$	$(2,1)$	$(2,2)$
1	0.238734	0.158710	—	—
2	0.234977	0.152966	0.146026	0.120879
3	0.235097	0.153740	0.143691	0.117171
4	0.235094	0.153785	0.143681	0.117137
5	0.235096	0.153792	0.143730	0.117331
6	0.235095	0.153794	0.143728	0.117331

TABLE 1. The first four eigenfrequencies σ_{nm}, where n is the transverse and m the along-axis wavenumber. Here $b = l = 1$. The rapid convergence with increasing truncation order N is evident.

N	$\lvert a_1\rvert$	$\lvert a_2\rvert$	$\lvert a_3\rvert$	$\lvert a_4\rvert$
4	1	1.958×10^{-1}	1.110×10^{-4}	6.728×10^{-7}
5	1	1.972×10^{-1}	1.045×10^{-4}	5.013×10^{-7}
6	1	1.963×10^{-1}	1.008×10^{-4}	2.739×10^{-7}
7	1	1.959×10^{-1}	1.000×10^{-4}	2.652×10^{-7}

TABLE 2. Convergence of selected coefficients a_i in (3.1) for σ_{12} with increasing truncation order N; $b = l = 1$

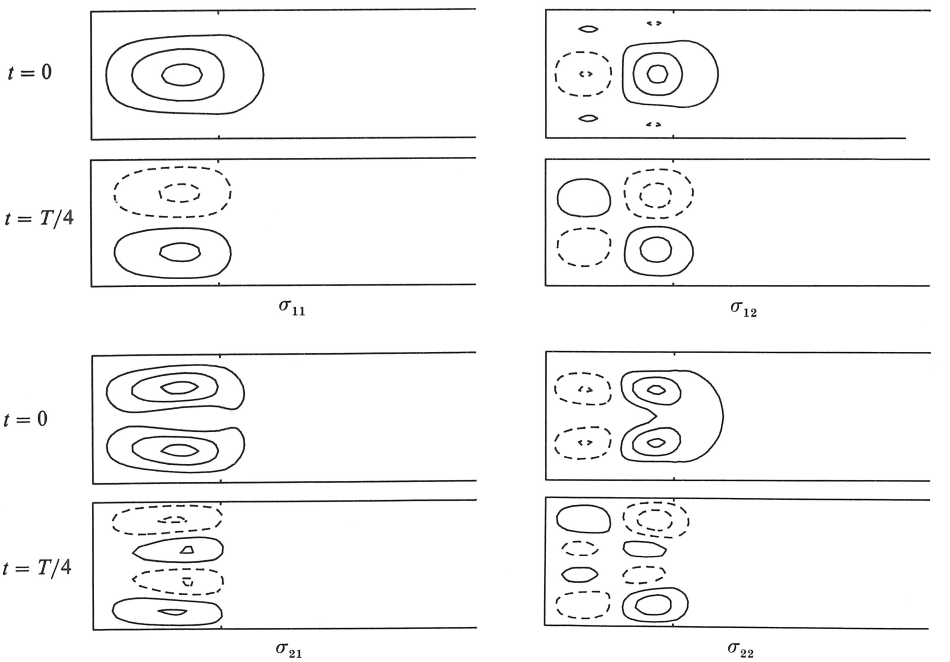

FIGURE 2. The stream function Ψ of the first four eigenfrequencies in a flat semi-infinite channel with a shelf bay zone. The solutions are bay modes: all wave activity is trapped in the bay zone and Ψ is exponentially evanescent for $x > l$. Here $b = l = 1$ and $N = 6$.

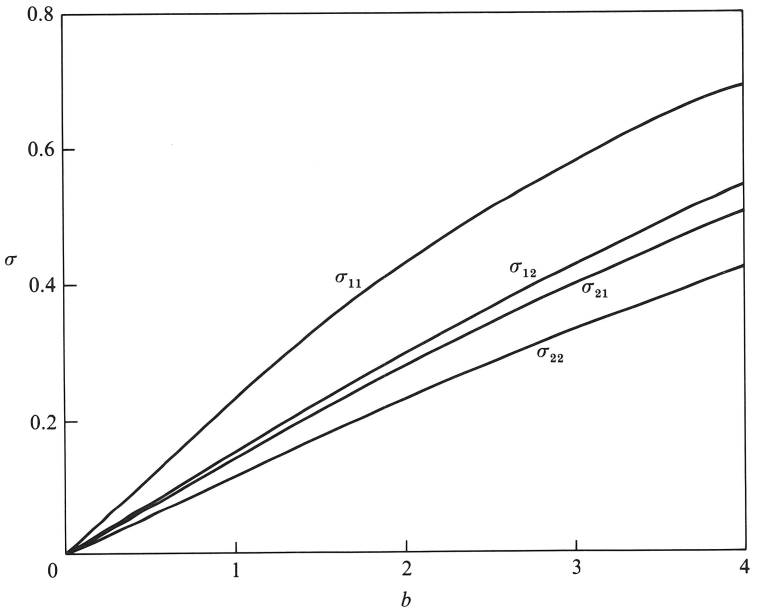

FIGURE 3. The eigenfrequencies σ as functions of the topography parameter b for $l = 1$, $N = 6$ for a bay adjacent to a flat semi-infinite channel.

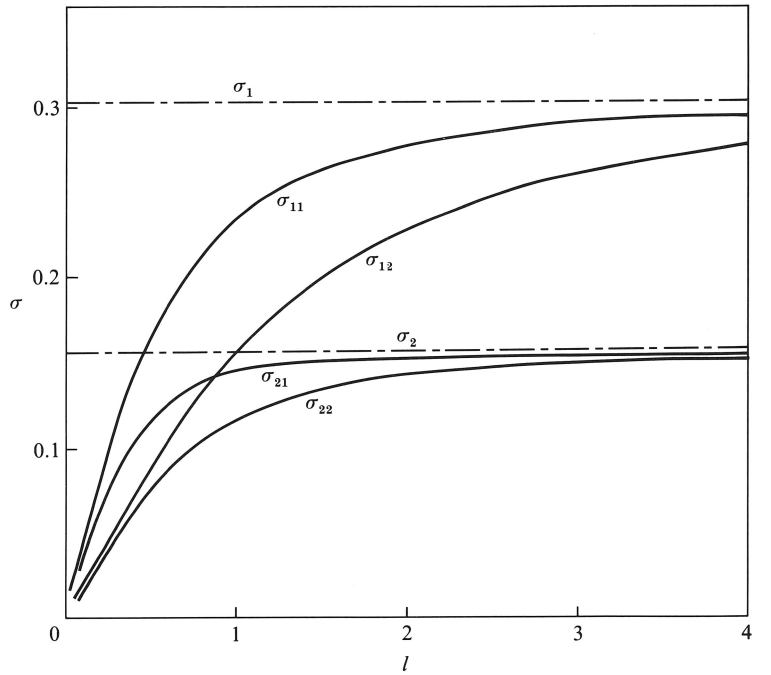

FIGURE 4. The eigenfrequencies σ as functions of the length l of the bay for $l = 1$, $N = 6$ for a bay adjacent to a flat semi-infinite channel.

Changing the topography parameter does not alter the ordering of the eigenfrequencies.

In figure 4 the eigenfrequencies are plotted as functions of l, the length of the bay. For large l they approach their corresponding cutoff and the frequencies of modes with different along-axis wavenumbers merge. For small l different transverse mode numbers are less important. Hence, the relative ordering of the modes changes with l. Large l will gather modes with identical transverse mode numbers whereas eigenfrequencies of modes with identical along-channel mode numbers merge for small l. This is in contrast to the behaviour shown in figure 3.

4. Channel with topography

Consider now (2.3) with $c \neq 0$. The cutoff frequencies σ_n given by (2.15) are non-zero and so for $\sigma < \sigma_1$ topographic waves carry energy both towards and away from the bay: only for $\sigma > \sigma_1$ are bay modes possible. The spectrum is *discrete* (or empty) above σ_1 and *continuous* below it.

It follows from (2.14) and (2.15) that for $\sigma < \sigma_{N_R}$, for any integer N_R, there are $2N_R$ propagating modes in the channel. N_R modes have positive group velocity and carry energy away from the bay. The remaining N_R modes carry energy towards the bay and any one of these can be selected as the incident wave ψ_i. For definiteness, attention is restricted to an incident wave of transverse order 1. Similar results are obtained for other incident modes. The solution takes the form

$$\psi = \begin{cases} \displaystyle\sum_{n=1}^{\infty} a_n \psi_n^{\mathrm{b}} = \mathrm{e}^{\beta x + \gamma y} \sum_{n=1}^{\infty} a_n \sinh \alpha_n x \sin n\pi y, \quad 0 \leqslant x \leqslant l, & (4.1a) \\ \psi_i^{\mathrm{c}} + \displaystyle\sum_{n=1}^{\infty} d_n \psi_n^{\mathrm{c}} = \mathrm{e}^{cy} \mathrm{e}^{\mathrm{i}k_i x} \sin \pi y \\ \qquad + \mathrm{e}^{cy} \displaystyle\sum_{n=1}^{N_R} r_n \mathrm{e}^{\mathrm{i}k_n x} \sin n\pi y \\ \qquad + \mathrm{e}^{cy} \displaystyle\sum_{n=N_R+1}^{N} d_n \mathrm{e}^{\mathrm{i}k_n x} \sin n\pi y, \quad x > l, & (4.1b) \end{cases}$$

$$k_i = \frac{c}{\sigma} + \left[c^2\left(\frac{1}{\sigma^2} - 1\right) - \pi^2\right]^{\frac{1}{2}},$$

$$k_n = \begin{cases} \dfrac{c}{\sigma} - \left[c^2\left(\dfrac{1}{\sigma^2} - 1\right) - (n\pi)^2\right]^{\frac{1}{2}}, & n \leqslant N_R, \\ \dfrac{c}{\sigma} + \mathrm{i}\left[(n\pi)^2 - c^2\left(\dfrac{1}{\sigma^2} - 1\right)\right]^{\frac{1}{2}}, & n > N_R. \end{cases} \qquad (4.2)$$

The solution (4.1) in the channel region consists of three contributions. The first represents the incident mode and the second the superposition of N_R reflected modes. The third contribution comprises the evanescent modes which are important only close to the bay zone. The latter two sums may be combined to a single term with $d_n \equiv r_n$ for $n = 1, \ldots, N_R$.

Requiring again continuity of ψ and ψ_x at $x = l$ gives

$$\left.\begin{aligned} \mathrm{e}^{\beta l+\gamma y}\sum a_n \sinh\alpha_n l \sin n\pi y &= \mathrm{e}^{cy}\,\mathrm{e}^{\mathrm{i}k_1 l}\sin\pi y + \mathrm{e}^{cy}\sum d_n\,\mathrm{e}^{\mathrm{i}k_n l}\sin n\pi y,\\ \mathrm{e}^{\beta l+\gamma y}\sum a_n(\beta\sinh\alpha_n l+\alpha_n\cosh\alpha_n l)\sin n\pi y &\\ = \mathrm{e}^{cy}\,\mathrm{i}k_1\,\mathrm{e}^{\mathrm{i}k_1 l}\sin\pi y + \mathrm{e}^{cy}\sum d_n\,\mathrm{i}k_n\,\mathrm{e}^{\mathrm{i}k_n l}\sin n\pi y.& \end{aligned}\right\} \tag{4.3}$$

Operating on both sides with $\int \mathrm{d}y\,\mathrm{e}^{-\gamma y}\sin m\pi y$ isolates the bay coefficients according to

$$\begin{aligned} \tfrac{1}{2}\mathrm{e}^{\beta l}a_m\sinh\alpha_m l &= e^{ik_1 l}J_{m1}+J_{mn}\,\mathrm{e}^{\mathrm{i}k_n l}d_n,\\ \tfrac{1}{2}\mathrm{e}^{\beta l}a_m(\beta\sinh\alpha_m l+\alpha_m\cosh\alpha_m l) &= \mathrm{i}k_1\,\mathrm{e}^{\mathrm{i}k_1 l}J_{m1}+J_{mn}\,\mathrm{i}k_n\,\mathrm{e}^{\mathrm{i}k_n l}d_n, \end{aligned} \tag{4.4}$$

where the sum over n is understood and J_{mn} is given in (3.5). Eliminating a_m from (4.4) yields the inhomogeneous algebraic system

$$(\mathrm{e}^{\mathrm{i}k_n l}(\beta+\alpha_m\coth\alpha_m l-\mathrm{i}k_n)J_{mn})\,d_n = (\mathrm{i}k_1-\beta-\alpha_m\coth\alpha_m l)\,\mathrm{e}^{\mathrm{i}k_1 l}J_{m1}, \tag{4.5}$$

which is truncated to order N when a numerical solution is sought.

4.1. *Bay modes*

When $\sigma > \sigma_1$ all modes are evanescent in the channel and trapped in the bay. The number of bay modes for a given geometry can be obtained using the frequency estimates of §2. Mode (n, m) is trapped if $\sigma^{\ell}_{nm} \geqslant \sigma_1$ and cannot be trapped if $\sigma^{\mathrm{u}}_{nm} \leqslant \sigma_1$. Let $N_{\mathrm{B}}(n)$ be the number of bay modes of transverse order n. Then from (2.15), (2.17) and (2.18)

$$[l(b^2/c^2+1-n^2)^{\frac{1}{2}}] \leqslant N_{\mathrm{B}}(n) \leqslant [\tfrac{1}{2}+l(b^2/c^2+1-n^2)^{\frac{1}{2}}], \tag{4.6}$$

where [ ] denotes the integer part. This relation determines $N_{\mathrm{B}}(n)$ uniquely when the bounds coincide and gives upper and lower estimates differing by unity otherwise.

The total number of bay modes follows as

$$N_{\mathrm{B}} = \sum_{n=1}^{\infty} N_{\mathrm{B}}(n). \tag{4.7}$$

If the channel is flat ($c = 0$), this series consists of an infinite number of terms corresponding to a doubly infinite set of bay modes. For $c > 0$ the series is finite, consisting of at most $[(b^2/c^2+1-1/(2l^2))^{\frac{1}{2}}]$ non-zero terms. Thus bay modes are absent if $c > 2bl$. A stronger criterion for the absence of bay modes is of course given by $\sigma^{\mathrm{u}}_{11} \leqslant \sigma_1$. Relation (4.7) gives straightforward bounds on the size of the spectrum, including the effects of both geometry and topography.

Bay modes for two values of c are displayed in figure 5. For $c = 0.3$ (4.7) yields $6 \leqslant N_{\mathrm{B}} \leqslant 8$ (3 are shown). For $c = 1$, $N_B = 1$ and only the fundamental bay mode is present. For $c \geqslant 1.55$, i.e. $\alpha^{\mathrm{u}}_{11} \leqslant \sigma_1$, no bay modes occur. Phase propagation in the bay zone follows the lines of constant depth and is therefore slanted according to the ratio bl/c.

4.2. *Reflections*

In this section the properties of the semi-infinite channel under incident wave energy are studied. This implies restriction of the frequency domain for which topographic wave propagation in the channel region is possible to the interval $0 < \sigma < \sigma_1$. This is the *continuous* part of the spectrum. The solution to this problem is given by the inhomogeneous algebraic system (4.5).

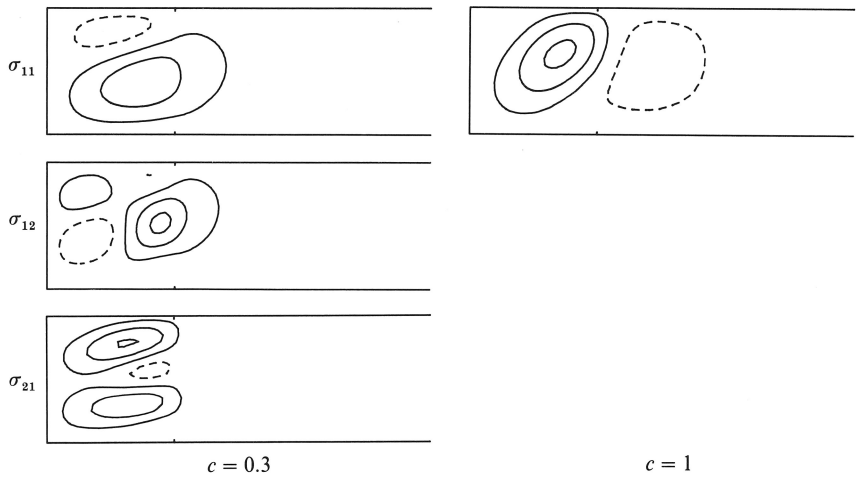

FIGURE 5. Contours of the stream function of the first three bay modes ($c = 0.3$) and the single bay mode ($c = 1$). The parameters are $b = l = 1$ and $N = 6$.

For $\sigma_{n+1} < \sigma < \sigma_n$ the reflected energy is distributed onto n different transverse modes. The relative importance of these modes can be determined by calculating the fluxes of kinetic energy associated with each of them.

With reference to the transport equation for kinetic energy density given in Part 1, define the time-averaged energy flux crossing any plane $x =$ constant in the channel by

$$\bar{\boldsymbol{F}} = \left\langle \int_0^1 \boldsymbol{F}\, dy \right\rangle. \tag{4.8}$$

This is independent of x as the time-averaged flux field is solenoidal and $\boldsymbol{F}$ vanishes on $y = 0, 1$. Recasting (2.3a) of Part 1 in terms of the complex wave amplitude ψ, and inserting (2.3) and (4.1b) gives the total flux (4.8) as the sum of the fluxes of the individual incident and reflected modes, viz.

$$F = F_{\mathrm{i}} + \sum_{n=1}^{\infty} F_n = \tfrac{1}{8} \mathrm{e}^{2c} \sum (2c - \sigma(k_n + k_n^*))\, \mathrm{e}^{\mathrm{i}(k_n - k_n^*)x}\, d_n\, d_n^*.$$

The wavenumbers for the propagating modes ($n = \mathrm{i}, 1, \ldots, N_{\mathrm{R}}$) and the evanescent modes ($n > N_{\mathrm{R}}$) are given in (4.2) and hence

$$F_n = \begin{cases} \tfrac{1}{4} \mathrm{e}^{2c} (c - \sigma k_n)\, r_n\, r_n^*, & n \leqslant N_{\mathrm{R}}, \\ 0, & n > N_{\mathrm{R}}. \end{cases} \tag{4.9}$$

The energy contained in the evanescent modes is locally conserved. Expression (4.9) suggests the introduction of a positive reflection coefficient R_n per unit incident energy flux of the form

$$R_n = \frac{c - \sigma k_n}{\sigma k_{\mathrm{i}} - c} |r_n|^2, \tag{4.10}$$

satisfying the relation

$$\sum_{n=1}^{N_{\mathrm{R}}} R_n = 1.$$

Figure 6 displays R_n as a function of the frequency. For the chosen channel topography ($c = 1$) the cutoff frequencies are $\sigma_1 = 0.3033$, $\sigma_2 = 0.1572$, $\sigma_3 = 0.1055$.

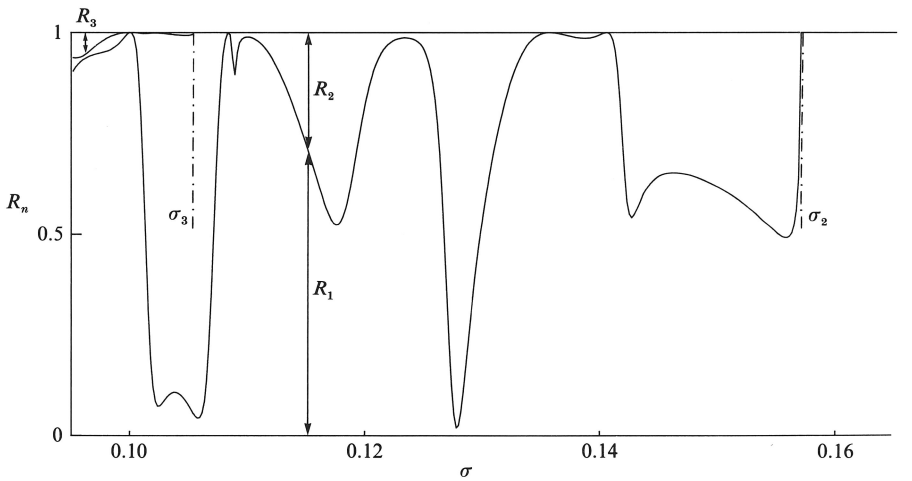

FIGURE 6. Reflection coefficients R_n as a function of the frequency. The parameters are $N = 6$, $b = c = l = 1$.

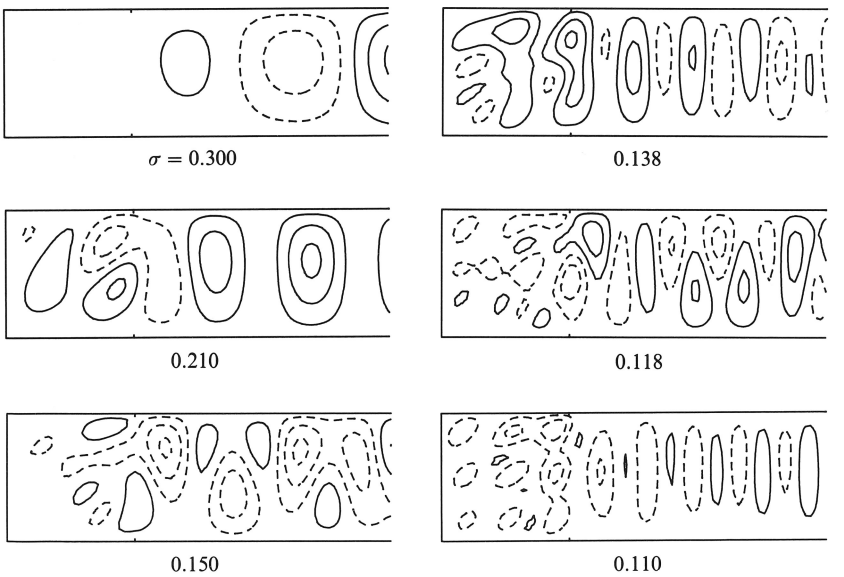

FIGURE 7. Streamlines for decreasing frequencies in the continuous spectrum. The parameters are as in figure 6.

For $\sigma_2 < \sigma < \sigma_1$ all reflected energy is contained in R_1 with $R_1 \equiv 1$. Decreasing σ below each successive cutoff frequency adds further reflected modes. Note that R_1 and R_2 contain alternately the major part of the reflected energy. Changes from one behaviour to the other are very sharp. Figure 6 is qualitatively similar to the corresponding figure in Stocker (1988) showing that the simple geometry of the present model captures the main features involved with the reflection of topographic waves.

Figure 7 shows solutions belonging to the continuous spectrum. For $\sigma_2 < \sigma < \sigma_1$ a beat pattern prevails in the channel part arising from a superposition of the incident wave with wavenumber k_i and the only reflected mode k_1, both of identical

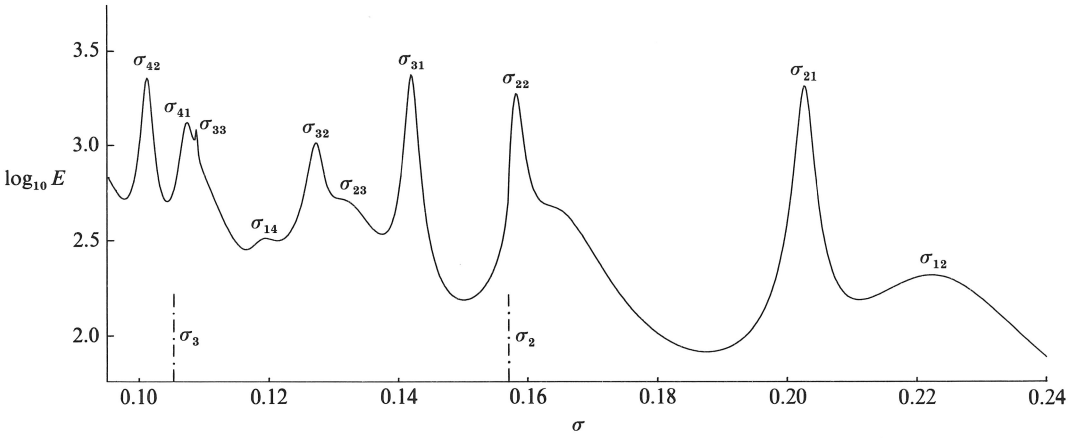

FIGURE 8. Energy in the bay as a function of the frequency. The parameters are as in figure 6.

transverse order. Note that for frequencies close to the cutoff σ_1 no wave energy can be fed into the bay zone. As the wavelength of the incident wave becomes shorter (for σ decreasing) wave activity in the bay is enhanced. For $\sigma < \sigma_2$ wave motion in the channel consists of several transverse modes. The reflection behaviour of the semi-infinite channel strongly depends on the frequency of the incident wave. This mode has the characteristic lengthscale $2\pi/k_i$ which interacts with the 'resonator' (the bay) of lengthscale bl/c.

4.3. *Bay modes and resonances*

Resonances in the continuous spectrum were reported by Stocker (1988) and associated with leaky bay modes. These are revealed in the present study by considering the energy content of the bay zone. The depth-integrated energy density per unit mass in terms of the complex stream-function amplitude over one period is

$$\langle e \rangle = \frac{\psi_x \psi_x^* + \psi_y \psi_y^*}{4H}. \tag{4.11}$$

Integrating (4.11) over the bay zone to obtain the total energy shows that the modes couple in the bay zone, in contrast to the modes in the channel, for which there is no interaction. The result, scaled on the incident flux, is

$$E = \frac{1}{2}\frac{e^{2bl}}{\sigma k_i - c}\left\{\sum_{n=1}^{\infty} a_n a_n^* s_n \left[\frac{1}{2\alpha_n}\sinh \alpha_n l(b^2+c^2+(n\pi)^2) - \frac{l}{\sigma^2}(b^2+c^2)+\frac{b}{2}(\cosh \alpha_n l - 1)\right] - 2i\frac{\pi b}{\sigma}\sum_{\substack{n,m \\ n\neq m}}^{\infty} a_n a_m^* \frac{nm}{n^2-m^2}(1-(-1)^{n+m})\mathcal{S}_{nm}\right\}, \tag{4.12}$$

where

$$s_n = \begin{cases} 1 & \text{for } \alpha_n^2 > 0, \\ -1 & \text{for } \alpha_n^2 < 0, \end{cases}$$

$$\mathcal{S}_{nm} = \frac{1}{\alpha_n + \alpha_m^*}\sinh(\alpha_n + \alpha_m^*)l - \frac{1}{\alpha_n - \alpha_m^*}\sinh(\alpha_n - \alpha_m^*)l.$$

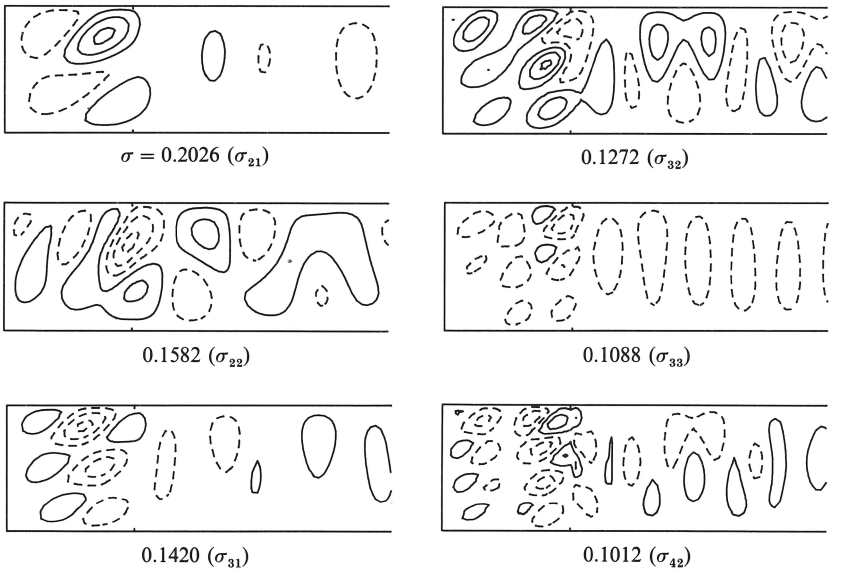

FIGURE 9. Streamlines at resonances corresponding to figure 8.

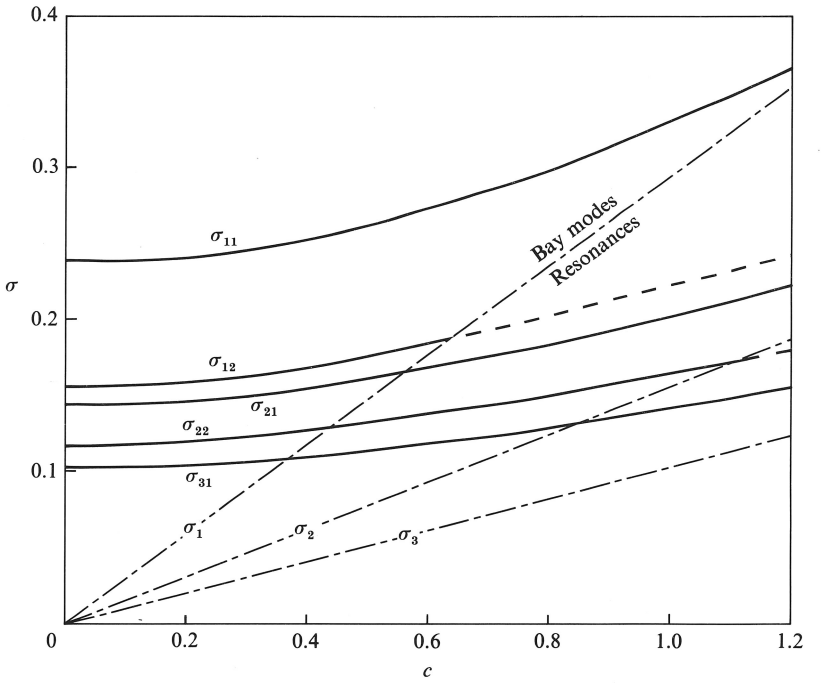

FIGURE 10. Frequencies of bay modes and resonances as functions of the channel topography. For increasing c the bay modes undergo transition to resonances. Thus each resonance in the continuous spectrum $\sigma < \sigma_1$ corresponds to a bay mode of the discrete spectrum for $c = 0$ (flat channel). The parameters are as in figure 6.

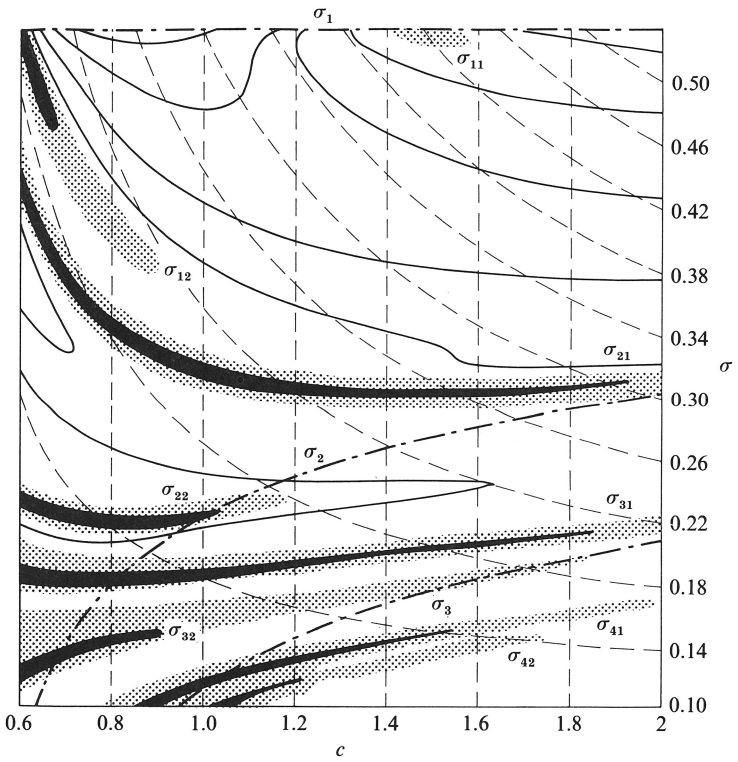

FIGURE 11. Lines of constant energy in the bay, increasing towards the shaded areas. The figure displays the domain $0.6 \leqslant c \leqslant 2$ and $0.1 \leqslant \sigma \leqslant \sigma_1$ of figure 10 mapped onto a square. Dashed lines of constant c are vertical, those of constant σ are curved; dashed-dotted lines indicate the cutoff frequencies of the adjacent channel. The resonances appear as ridges in this graph and are labelled according to their bay-mode limit for $c = 0$. Resonances σ_{nm} become weak when $\sigma_{nm} < \sigma_n$.

Figure 8 displays the total amount of energy as a function of the incident frequency. Whereas the reflection coefficient revealed no structure in $\sigma_2 < \sigma < \sigma_1$, the bay energy exhibits a conspicuous resonance at $\sigma = 0.203$. At $\sigma = 0.222$ a further weak resonance is visible. This indicates that each resonance can be associated with a pair of mode numbers according to the structure of the wave motion in the bay zone. From figure 9 it is evident that the bays sustain patterns very much like those shown in figure 5 which were true bay modes.

It has been demonstrated above that the spectrum of the topographic wave equation in the semi-infinite channel can consist of a discrete and a continuous spectrum. Solutions associated with the discrete spectrum are trapped in the bay zone – they are true bay modes whereas solutions of the continuous part are free states: incoming wave energy is reflected. Increasing the cutoff frequency of the channel region, i.e. increasing c, causes a decrease in the number of true bay modes. Figure 10 displays the bay mode frequencies as functions of the topography parameter c. The dashed-dotted lines indicate the cutoff frequencies of the individual transverse modes. For $\sigma < \sigma_1$ true bay modes evolve. It is evident that, owing to a different functional dependence of σ_n and σ_{nm} with respect to c, the lines of σ_{nm} intersect those of σ_n for increasing c. Once σ_1 is crossed a true bay mode becomes a resonance in the continuous spectrum. Moreover, once σ_{nm} crosses σ_n the resonance

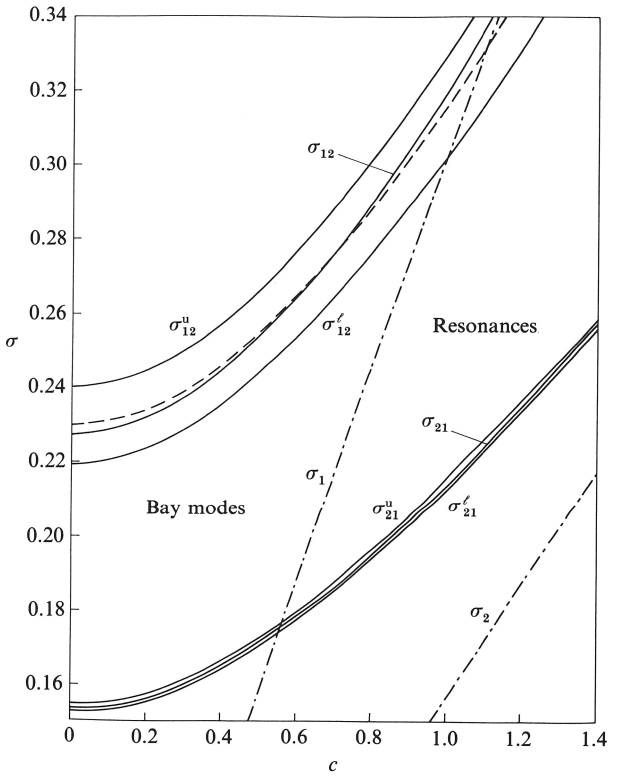

FIGURE 12. Upper and lower bounds for the eigenfrequencies σ_{12} and σ_{21} and their average (dashed line) as functions of the channel topography. The cutoff frequencies σ_1 and σ_2 are dashed-dotted. For $\sigma < \sigma_1$ bay modes prevail and the bounds are rigorous. For the strong resonance $\sigma_{21} < \sigma_1$ the estimated frequency is still good, whereas deviations are observed as the resonance becomes weak, i.e. $\sigma_{12} < \sigma_1$. The parameters are $N = 6$, $b = 1$, $l = 2$.

may become weak, because the mode with the same transverse mode number n is now propagating in the channel. This is indicated by dashed lines in the figure. Therefore, each resonance in the continuous spectrum can be associated to a true bay mode, i.e. a solution of the discrete spectrum of the simple bay model with $c = 0$. Hence, with increasing c (or decreasing bl) true bay modes do not vanish but rather emerge as resonant states in the continuous spectrum.

Figure 11 displays more quantitatively the development of the resonances when the leakage of the adjacent channel is increased. The domain $0.6 \leqslant c \leqslant 2$ and $0.1 \leqslant \sigma \leqslant \sigma_1$ of figure 10 is mapped onto a square and lines of constant bay energy are plotted. Resonances appear as shaded ridges; they are labelled according to their flat-channel limit. Once the resonance σ_{nm} falls below the cutoff σ_n the energy in the bay decreases and the resonance becomes weak.

In §2 lower and upper bounds of the eigenfrequency σ_{nm} were calculated. Figure 12 displays these bounds for the two $(1,2)$ and $(2,1)$ modes as a function of the channel topography. The exact value lies close to the average of the bounds, being graphically indistinguishable for the $(2,1)$ mode and differing by less than 1 % for the $(1,2)$ mode. The accuracy of the estimates relies on the assumption that the majority of the disturbance is confined to the bay zone. Thus the estimate remains good for the $(2,1)$ mode below the frequency σ_1 at which propagating modes occur in

	Structure of domain	Discrete spectrum	Continuous spectrum
1.	Lake basin, domain closed	Countably infinite	Empty
2.	Bay zone connected with flat open domain	Countably infinite	Empty
3.	Open domain: bay and adjacent channel or shelf with cutoff σ_1	Finite for $\sigma > \sigma_1$	$0 < \sigma < \sigma_1$, infinite number of resonances
4.	As 3 with σ_1 large	Empty	$0 < \sigma < \sigma_1$, infinite number of resonances
5.	No bay zone or bay conformally equivalent to channel	Empty	$0 < \sigma < \sigma_1$, no resonances

TABLE 3. The structure of the domain governs the spectrum

the channel and the mode becomes a strong resonance. The estimate is poorer for the mode $(1, 2)$ below the frequency σ_1 as the resonance is only weak and so the disturbance in the channel is relatively strong.

5. Conclusions

Topographic waves in a semi-infinite channel with a terminating bay zone are considered. Solutions are given in both the bay and channel regions by a linear superposition of modes of increasing transverse order. The coefficients involved are calculated by solving a homogeneous system of linear algebraic equations that emerge from stating continuity of the physically relevant fields across the bay edge. In order to obtain numerical solutions, the infinite dimensional system is truncated; convergence of both eigenvalues and eigensolutions is demonstrated. Truncation orders as small as three provide satisfactory results for the lowest modes.

A first simple configuration consists of a shelf bay zone adjacent to a flat channel. This prevents wave energy from radiating away from the bay: waves are trapped. It is shown that this geometry sustains a countably infinite set of bay modes – solutions which are exponentially evanescent away from the bay. The spectrum of eigenfrequencies is discrete. These solutions are in qualitative agreement with the bay modes of Stocker & Hutter (1987*a*, *b*).

To more closely model their results the topography was generalized to consider a channel with a shelf and a bay with oblique bottom contours. The number of bay modes was shown to be of the order bl/c, thus reflecting the interplay of the topography (b, c) and geometry (l) of the domain. Whereas the spectrum of the flat channel is purely discrete, channels with transverse topography exhibit compound spectra consisting of a continuous and a possibly empty, discrete part. The former contains an infinite set of resonances each of which can be attributed to a point in the discrete spectrum of the flat channel. Resonances can thus be considered as leaky bay modes. Table 3 summarizes these findings.

It is apparent that solutions that belong to the discrete part of the spectrum represent an important and characteristic feature of topographically trapped waves. This study therefore strongly suggests that one should be aware of localized wave motion in domains with variable cutoff frequencies of topographic Rossby waves, such as gulfs and estuaries connected to continental shelves or bays in lakes.

Generally, in a lake or ocean basin each bay or localized topographic irregularity may sustain its own trapped modes or can be brought into resonance by an external

source such as shelf waves along continental boundaries or passing atmospheric systems. It is the local geometry and the particular topography that determines the frequency of the bay modes and resonances. The topography of adjacent shelves is decisive in whether wave energy in the bay can be carried away forming a leaky mode or whether the mode remains trapped.

One of the authors (T.F.S.) was supported by SERC grant GR/E/64039 while performing this study. This and the typing of B. R. Lankester is gratefully acknowledged.

REFERENCES

BALL, F. K. 1965 Second class motions of a shallow liquid. *J. Fluid Mech.* **23**, 545–561.

JOHNSON, E. R. 1987*a* Topographic waves in elliptical basins. *Geophys. Astrophys. Fluid Dyn.* **37**, 279–295.

JOHNSON, E. R. 1987*b* A conformal mapping technique for topographic wave problems: semi-infinite channels and elongated basins. *J. Fluid Mech.* **177**, 395–405.

JOHNSON, E. R. 1989 Topographic waves in open domains. Part 1: Boundary conditions and frequency estimates. *J. Fluid Mech.* **200**, 69–76.

LAMB, H. 1932 *Hydrodynamics*, 6th edn. Cambridge University Press.

MYSAK, L. A. 1985 Elliptical topographic waves. *Geophys. Astrophys. Fluid Dyn.* **31**, 93–135.

MYSAK, L. A., SALVADE, G., HUTTER, K., SCHEIWILLER, T. 1985 Topographic waves in an elliptical basin, with application to the Lake of Lugano. *Phil. Trans. R. Soc. Lond.* A **316**, 1–55.

RHINES, P. B. 1969*a* Slow oscillations in an ocean of varying depth. Part 1. Abrupt topography. *J. Fluid Mech.* **37**, 161–189.

RHINES, P. B. 1969*b* Slow oscillations in an ocean of varying depth. Part 2. Islands and seamounts. *J. Fluid Mech.* **37**, 191–205.

RHINES, P. B. & BRETHERTON, F. 1973 Topographic Rossby waves in a rough-bottomed ocean. *J. Fluid Mech.* **61**, 583–607.

STOCKER, T. 1988 A numerical study of topographic wave reflection in semi-infinite channels. *J. Phys. Oceanogr.* **18**, 609–618.

STOCKER, T. & HUTTER, K. 1986 One-dimensional models for topographic Rossby waves in elongated basins on the *f*-plane. *J. Fluid Mech.* **170**, 435–459.

STOCKER, T. & HUTTER, K. 1987*a* Topographic Waves in Channels and Lakes on the *f*-Plane. Lecture Notes on Coastal and Estuarine Studies, Vol. 21. Springer.

STOCKER, T. & HUTTER, K. 1987*b* Topographic waves in rectangular basins. *J. Fluid Mech.* **185**, 107–120.

TRÖSCH, J. 1984 Finite element calculation of topographic waves in lakes. *Proc. 4th Intl Conf. Appl. Numerical Modeling. Tainan, Taiwan* (ed. Han Min Hsia, You Li Chou, Shu Yi Wang & Sheng Jii Hsieh), pp. 307–311.